RSC Advances

ROYAL SOCIETY OF CHEMISTRY

www.rsc.org/advances

Facile Synthesis of Litchi Shaped Cuprous Oxide and Its Application for Aerobic Oxidative Synthesis of Imines

Nearly uniform litchi shaped cuprous oxide (Cu_2O) nanoaggregate was readily synthesized in the absence of surfactants or templates. The as-obtained Cu_2O nanoaggregates were well characterized and they showed efficiently catalytic activities in aerobic oxidative synthesis of imines.

RSC Advances

RSC Publishing

ARTICLE

Facile Synthesis of Litchi Shaped Cuprous Oxide and Its Application for Aerobic Oxidative Synthesis of Imines

Cite this: DOI: 10.1039/xoxxooooox

Received ooth January 2012,
Accepted ooth January 2012

DOI: 10.1039/xoxxooooox

www.rsc.org/

Lei Bai,[a,b *] and Zheng Dang[c]

In the present work, uniform litchi shaped cuprous oxide (Cu_2O) nanoaggregates were synthesized via a facile method by employing copper(II) chloride, sodium hydroxide, ethylene glycol and ascorbic acid in the absence of surfactants at room temperature. With further increase of the reaction temperature, broken hollow copper nanoaggregates were obtained. The structure of Cu_2O nanoaggregate was characterized by X-ray diffraction (XRD), scanning electron microscope (SEM), X-ray photoelectron spectroscopy (XPS), Transmission Electron Microscopy (TEM), Brunauer–Emmett–Teller (BET) analysis and High Resolution Transmission Electron Microscopy (HRTEM). The as-obtained Cu_2O nanoaggregates showed efficiently catalytic activities in aerobic oxidative synthesis of imines.

Introduction

Nanomaterials, as well recognized, show enhanced properties and have a variety of potential applications in catalysis, biosensors and nanoelectronics. Besides, the use of nanomaterials could be affected by their size, morphology and structure.[1-2] To obtain nanomaterials with controllable structures, various methods have been developed.[3] Generally, both surfactants such as polyvinylpyrrolidone and hard templates such as ordered structural carbon have been adopted in order to optimize the dimension, direction and morphology.[4,5] In the meantime, self-assembled nanomaterials also attract a great deal of interests.[3c]

Cuprous oxide (Cu_2O), which is a non-stoichiometric defect p-type semiconductor, has been widely applied in several fields such as CO oxidation, organic synthesis, antibacterial activity, photocatalysis, gas sensor, solar driven water splitting and solar energy conversion.[6-9]

Size- and morphology-dependent properties of Cu_2O such as the size-dependent color exhibition require better controlling the growth of nanocrystals in the synthesis strategy.[10] Nanocubes, nanowires, nanospheres, hollow structures and various polyhedra (with different number of facets) of Cu_2O have been successfully obtained with the assistance of polymers and surfactants.[11-14] The presence of surfactants and polymers in the preparation of Cu_2O nanostructures can more precisely control the growth of nanocrystals as well as modify the surfaces of the crystals to be fit for dispersing in different solvents.[14] On the other hand, surfactant-free synthesis of nanomaterials could provide crystals having a relatively clean surface but with a large size.[3c,d] Thus, the synthesis of uniform nanostructures of Cu_2O in several hundred nanometers (below 200 nm) by facile methods with low-cost of materials and low energy-consumption is still a hot topic from the view of both the fundamental research and applications in potential..

Herein, we report the synthesis of a novel litchi shaped Cu_2O nanoaggregates (~100 nm) by the use of copper (II) chloride, sodium hydroxide, ethylene glycol (EG) as solvent and ascorbic acid (AA) as the reducing agent at room temperature without employing any polymers or surfactants. Furthermore, by increasing the temperature, broken hollow Cu nanoaggregates are obtained possibly due to the further reduction of Cu_2O. The structure of the nanoaggregates is well characterized and finally, the obtained Cu_2O nanoaggregates have been found inspiring applications in aerobic oxidative synthesis of imines.

Experimental

Synthesis of Cu_2O nanoaggregates: All the reagents were used as received without further purifications. In a typical synthesis, 1 mmol $CuCl_2 \cdot 2H_2O$ and 8 mmol sodium hydroxide were added into 10 mL EG and stirred until a dark blue solution was obtained. Then, 2 mmol of AA solid were added into the above solution directly and kept stirring for desired time at room temperature. Finally, the yellow product was washed by distilled water and ethanol and dried under vacuum for further use.

Characterizations: X-ray diffraction (XRD) patterns were recorded on MiniFlex 600, Rigaku. X-ray photoelectron

spectroscopy (XPS) analysis was performed with a Thermo ESCALAB 250 instrument with a monochromatic Al Ka ($h\nu$ =1486.6 eV) X-ray source. Field emission scanning electron microscopy (FE-SEM) analysis was performed on JEOL JSM-7500B at 10 kV. The morphologies of nanocrystals were examined by transmission electron microscopy (TEM), using a JEOL JEM-2010 LaB6 high-resolution transmission electron microscope operated at 200 kV. The electron diffraction and HRTEM were performed on JEOL JEM-ARM200F, which was operated at 200 kV.

Brunauer–Emmett–Teller (BET) nitrogen-sorption data were obtained with a MicromeriticsTristar 3000 automated gas adsorption analyzer. Nuclear magnetic resonance hydrogen spectra (^{1}H NMR) were recorded on Avance III plus 400MHz. Ultraviolet–visible spectra were recorded on SHIMADZU UV–3600 spectrophotometer.

Synthesis of imines: In our case, for a typical reaction, 1 mmol of aromatic alcohol, 1.2 mmol of amine, 5 mmol% of Cu_2O with 1.5 mmol of KOH were added into 25 mL reactor pre-charged with 1 mL toluene and the reaction was kept at 343 K for 19 h. The conversion was confirmed by ^{1}H NMR with 1,4-dioxane as an internal standard.

Results and discussions

First of all, after washing and dispersing in ethanol, a brown-yellow sample is obtained as displayed in Figure 1. The sample is then dropped in a piece of glass, dried and characterized by XRD.

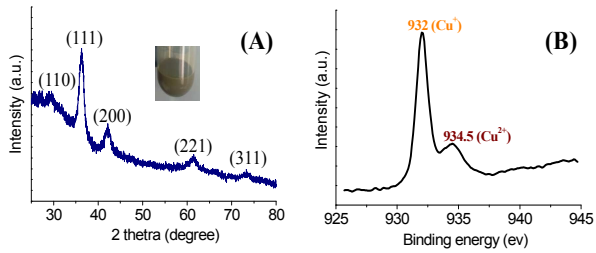

Figure 1. Representative XRD pattern of Cu_2O specie (A, inset, the photo of the sample) and the XPS spectrum of Cu_{2p} (B).

As shown in Figure 1A, the peaks at 29.5, 36.4, 42.1, 61.2 and 73.4^o corresponding to the crystal face of (110), (111), (200), (221) and (311), clearly suggests the formation of Cu_2O (ICSD No. 063281).

In order to further determine the chemical composition of the Cu_2O nanoaggregates, X-ray photoelectron spectroscopy (XPS) is performed and the XPS spectrum of Cu 2p exhibits two peaks at 932 and 934.5eV in Figure 1B, corresponding to the Cu $2p_{3/2}$ spin–orbit peaks of Cu^+ and Cu^{2+}, respectively. As displayed in the Figure, most species of the nanoaggregate are Cu^+ species. The specie of Cu^{2+} possibly occurred due to the oxidation of Cu^+ on the surface of Cu_2O nanoaggregates and this phenomenon is also observed in the case of Cu_2O-GNS.[15] However, the XRD pattern confirms that the sample still remains in Cu_2O phase as discussed above.

Furthermore, the size and morphology of the samples are characterized by SEM and TEM. As displayed by Figure 2A, it is shown that by using EG as solvent, the Cu_2O nanoaggregates have a litchi shaped structure and it is suggested from the images that the surface of the nanoaggregates, with a ~100 nm in diameter, is coarse and the litchi shaped nanoaggregate is composed by small particles (inset of Figure 2A). TEM image in Figure 2B further confirms that the nanoaggregates are composed by a different amount of small particles. The result of particle-size analysis shows that the small particles are about 5−11 nm as displayed in Figure 2C based on the calculation of one hundred particles. In addition, the BET specific surface area of nanoaggregates is 28.2 $m^2 \cdot g^{-1}$ (see SFigure 1).

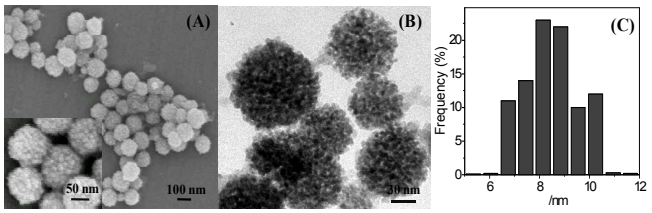

Figure 2. SEM (A), TEM (B) images of Cu_2O nanoaggregates and size distribution of Cu_2O nanoparticles (C) in the nanoaggregates.

In Figure 3A, the electron diffraction of a nanoaggregate (shown in the inset) is displayed, indicating that the nanoaggregates are polycrystalline. The formation of polycrystalline Cu_2O nanoaggregates is possibly due to the fact that in the absence of surfactants, small Cu_2O nanoparticles form in EG and assemble with each other quickly into nanoaggreates without a preferential growth face. The growth process of Cu_2O nanoaggregates would be studied in the following. A HRTEM image is displayed in Figure 3B and a part of the nanoaggregate shows a square pattern, indicating that it is aligned to [001] direction. The (200) and (110) plane spacings are measured to be 0.214 and 0.302 nm respectively, which are very close to the previously reported values,[16] further confirming the existence of Cu_2O.

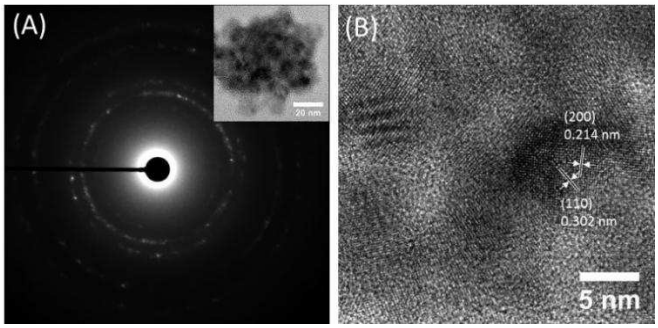

Figure 3. Electron diffraction (A) and high resolution TEM image (B) of the Cu_2O nanoaggregate.

The influence of the reaction time on the structures of Cu_2O nanoaggregates is also investigated. When the synthesis was stopped at 5 min, the TEM image of the product in Figure 4A suggests that the nanoaggregates formed by small particles with obvious voids are obtained with a relatively large range of diameter. With the increase of the reaction time, for the sample taken at 60 min (Figure 4B), its structure is similar as that obtained at 120 min, suggesting that the particles are assembled with each other to form relatively solid spherical aggregates. According to the above observations Figure 4, after adding AA, due to the steric effect of EG molecules, spherical Cu_2O nanoaggregates with many voids in the interior of spheric structure form quickly to reduce the surface energy. These

aggregated Cu_2O nanostructures are not in thermodynamically equilibrium status because of the quite large surface energy.[12a] Thus, after a certain time, relatively solid nanoaggreates are obtained and no obvious changes in the size of nanoaggregates are noticed between 60 min and 120 min.

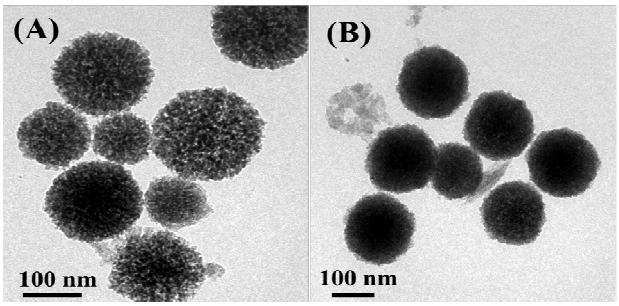

Figure 4. TEM images of Cu_2O nanoaggregates obtained at different reaction time (A) 5 and (B) 60 min.

More interestingly, when the reaction is further carried out at 353 K for 120 min, broken litchi shaped copper specie is formed as displayed in Figure 5 and also confirmed by XRD (see SFigure 2). The enhanced temperature increases the reducing ability of AA and it is shown that the increase of reaction temperature also enlarge the size of the aggregates up to 330 nm due to the absence of stabilizers.

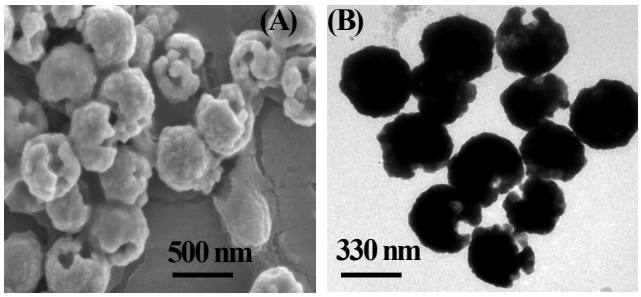

Figure 5. SEM and TEM images of copper nanoaggregates obtained at 353 K for 2 h.

The whole process of the synthesis is summarized in Scheme 1. It is proposed that under strongly basic conditions, a part of EG molecules can be transformed into anions that coordinated with copper ions to form Cu^{2+}–EG complexes as well as play a role in controlling the aggregation. By introducing AA, this kind of complex is reduced and transformed into Cu_2O species at room temperature. With the enhanced temperature, the AA molecules adsorbed on Cu_2O nanoaggregates or in the solution further reduce the nanoaggregates, which leads to a corrosion of Cu_2O as well as the formation of copper specie.

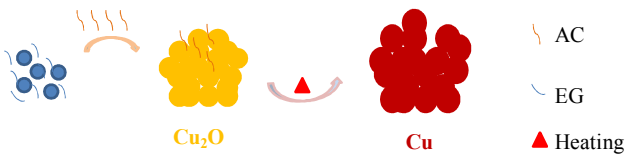

Scheme 1. Proposed mechanism of the formation of Cu_2O and Cu nanoaggregates.

After the investigation of the formation of Cu_2O nanoaggregates, the nanoaggregates are employed as a catalyst in the aerobic oxidative synthesis of imines. Imines with a reactive C=N bond can undergo different types of reactions such as reduction, cycloaddtion and addition as well as be versatile intermediates for nature products and biochemical active compounds.[17-19]

As shown in Table 1, when Cu_2O and KOH is used separately in the reaction with benzyl alcohol and benzylamine, the conversions of 74% and 18% imines are observed, indicating the catalytic ability of Cu_2O. In the same reaction, the conversion of the formation of imine is increased to 95% in the presence of both Cu_2O and KOH (entry 3). Moreover, the reuse of the catalyst in entry 3 with KOH, the conversion is still up to 78% for imines formation (entry 4). From these data, we reason that the Cu_2O nanoaggregate is an efficient catalyst for promoting the formation of imines.

Table 1. The performances of Cu_2O nanoaggregates on aerobic oxidative synthesis of imines.

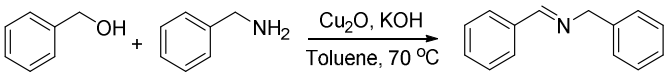

Entry		Conv. (%)
1	KOH only	18
2	Cu_2O only	74
3	KOH and Cu_2O	95
4	Reused of 3	78

Reaction conditions: benzylalcohol (1 mmol), benzylamine (1.2 mmol), KOH (1.5 mmol) and Cu_2O (5 mmol%) were added into toluene (1 mL) in a reactor and stirred for 19 h with an oxygen balloon. The formation and conversion of imines were confirmed by ^1H NMR and based on the consumption of aromatic alcohol.

With the obtained results, we then try to explore some other substrates and the results are listed in Table 2. For aniline and benzyl alcohol, the conversion of the imine formation is 85% (entry 1 of Table 2). The influence of functional groups of aniline as an example is investigated when benzyl alcohol is fixed.

As shown in Table 2, for *p*-Methoxyaniline and *o*-Methoxyaniline, a big difference in conversion (44%) of its corresponding imine is observed by the results in entry 2 and 4, suggesting that the steric effect has a significant influence on the conversion. While for *p*-Methoxyaniline and *p*-Toluidine, the difference in imine conversion could be resulted from the different ability in electron donating. A close conversion of the formation of imines between *m*- and *p*-Toluidine is found in comparison with the aniline itself. In addition, for electron attractive group such as bromine, a low conversion (54%) which is close to that of *o*-Methoxyaniline is obtained as displayed in entry 7, possibly due to that bromine is a smaller group. For aliphatic amines, conversions of 78 and 91% for the formation of imines between propylamine, laurylamine and benzyl alcohol are also observed, respectively. On the other hand, as for the modification of benzyl alcohol, good conversions of imines are obtained for 4-chlorobenzyl alcohol and 4-methylbenzyl alcohol. However, it is worth noting that this catalyst is not efficient when pyridin-3-ylmethanol is used, possibly due to the difficulty in oxidation of pyridin-3-ylmethanol (entry 12).

Table 2. Extension of the catalytic abilities of Cu_2O nanoaggregates on aerobic oxidative synthesis of imines.

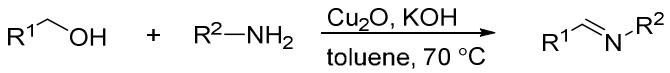

Entry	R^1	R^2	Conv. (%)
1	C_6H_5	C_6H_5	85
2	C_6H_5	4-$MeOC_6H_4$	94
3[a]	C_6H_5	4-$MeOC_6H_4$	96
4	C_6H_5	2-$MeOC_6H_4$	50
5	C_6H_5	4-MeC_6H_4	84
6	C_6H_5	3-MeC_6H_4	84
7	C_6H_5	2-BrC_6H_4	54
8	C_6H_5	$CH_3(CH_2)_2$	74
9	C_6H_5	$CH_3(CH_2)_{10}$	91
10	4-MeC_6H_4	$C_6H_5CH_2$	80
11	4-ClC_6H_4	$C_6H_5CH_2$	74
12	3-Py	$C_6H_5CH_2$	24

Reaction conditions: alcohol (1 mmol), amine (1.2 mmol), KOH (1.5 mmol), Cu_2O (5 mmol%) were added into toluene (1 mL) in a reactor and stirred for 19 h with an oxygen balloon. The formation and conversion of imines were confirmed by ^1H NMR and based on the consumption of alcohol. [a] another batch of Cu_2O.

For the formation of imines, it is proposed that first the aromatic alcohol is oxidized into aldehyde from previous work[20] and then condensation reaction between the two regents occurs as proposed in Scheme 2.

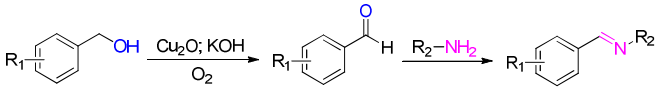

Scheme 2. Possible reaction path of the formation of imines.

It is known that Cu_2O is easy to be oxidized as evidenced by XPS results above. After the reaction in our experiments, the catalyst, Cu_2O nanoaggregate is investigated by XRD to find the changes of its structure and it is suggested that the Cu_2O species has been oxidized into CuO species as displayed in SFigure 3 after comparing with that of Cu_2O. Taking into account of the catalytic results (entry 1, 2, 3 as well as 4 in Table 1), it is reasonable that Cu_2O is the active phase for the synthesis of imines and more efficient than CuO. In addition, the leaching of the catalyst during the reaction is also investigated by extracting and analyzing the reaction solution. As shown by UV-Vis spectra in SFigure 4, in contrast with the spectrum of Cu^{II} solution, no Cu^{II} species are detected from the reaction solution. Based on the observations from SFigure 4 and the leaching experiments, it is confirmed that the transformation of catalysts occurs and no loss of copper is noticed. Thus, according to the above results, the further work could be focused on the comparison of the effect between CuO and Cu_2O on the aerobic synthesis of imines.

Conclusions

In conclusion, we had developed litchi shaped Cu_2O nanoaggregates by using EG and AA at room temperature in the absence of any templates or surfactants. The nanoaggregate was composed by ultra-small particles (5-11 nm in size) as evidenced by SEM and TEM results. The structure of the nanoaggregates was characterized by XRD, XPS, HRTEM and BET. Interestingly, broken litchi shaped Cu nanoaggregate was obtained at a higher temperature. The as-obtained Cu_2O was an efficient catalyst in the aerobic oxidative synthesis of imines. This work could provide a new insight for the synthesis of nanomaterials and their applications in organic synthesis.

Acknowledgments

Professor Y. D. Li and Professor Y. B. Kang are greatly appreciated for the financial support and useful advice. China Postdoctoral Science Foundation (No. 2014M561829) was greatly appreciated for the financial support. Hai Nan Natural Science Foundation (No.213028) was also appreciated for the financial support.

Notes and references

[a] Centre of Advanced Nanocatalysis, University of Science and Technology of China, Hefei, Anhui, China, 230026 E-mail: leibai@ustc.edu.cn, baileixy2007@163.com.
[b] Department of Chemistry, University of Science and Technology of China, Hefei, Anhui, China, 230026.
[c] Technique centre of Hai Nan Entry-Exit inspection and Quarantine Bureau

Electronic Supplementary Information (ESI) available: See DOI: 10.1039/b000000x/

1. Y. Wu, D. S. Wang and Y. D. Li, *Chem. Soc. Rev.*, 2014, **43**, 2112–2124.
2. (a) C. M. Cobley, J. Y. Chen, E. Chul Cho, L. H. V. Wang and Y. N. Xia, *Chem. Soc. Rev.*, 2011, **40**, 44–56; (b) A. Albanese, P. S. Tang and W. C. W. Chan, *Annu. Rev. Biomed. Eng.*, 2012, **14**, 1–16.
3. (a) X. Wang, J. Zhuang, Q. Peng and Y. D. Li, *Nature*, 2005, **437**, 121–124; (b) A. R. Tao, S. Habas and P. D. Yang, *Small*, 2008, **4**, 310–325. (c) W. Z. Wang, P. C. Zhang, L. Peng, W. J. Xie, G. L. Zhang, Y. Tu and W. J. Mai, *Cryst. Eng. Comm.*, 2010, **12**, 700–701. (d) S. D. Sun, F. Y. Zhou, L. Q. Wang, X. P. Song and Z. M. Yang, *Cryst. Growth Des.*, 2010, **10**, 541–547.
4. Z. D. Lu and Y. D. Yin, *Chem. Soc. Rev.*, 2012, **41**, 6874–6887.
5. F. Goettmann, A. Fischer, M. Antonietti and A. Thomas, *Angew. Chem. Int. Ed.*, 2006, **45**, 4467– 4471.
6. (a) K. Jayaramulu, V. M Suresh, and T. Kumar Maji, *Dalton Trans.*, 2015, **44**, 83-86; (b) J. T. Zhang , J. F. Liu , Q. Peng , X. Wang and Y. D. Li, *Chem. Mater.*, 2006, **18**, 867–871; (c) Z. L. Zhang, H. W. Che, J. J. Gao, Y. L. Wang, X. L. She, J. Sun, P. Gunawan, Z. Y. Zhong and F. B. Su, *Catal. Sci. Technol.*, 2012, **2**, 1207–1212.
7. (a) S. D. Sun, X. P. Song ,Y. X. Sun, D. C. Deng and Z. M. Yang, *Catal. Sci. Technol.*, 2012, **2**, 925–930.
(b) P. E. de Jongh, D. Vanmaekelbergh and J. J. Kelly, *Chem. Commun.*, 1999, 1069–1070.
8. A. Correa and C. Bolm, *Adv. Synth. Catal.*, 2007, **349**, 2673–2676.
9. (a) W.-C. Huang, L. M. Lyu, Y. C. Yang and M. H. Huang, *J. Am. Chem. Soc.*, 2012, **134**, 1261–1267; (b) M. Leng, M. Z. Liu, Y. B. Zhang, Z. Q. Wang, C. Yu, X. G. Yang, H. J. Zhang and C. Wang, *J. Am. Chem.* Soc.,2010, **132**, 17084–17087.
10. K. Borgohain, N. Murase and S. Mahamuni, *J. Appl. Phys.*, 2002, **92**, 1292–1297.
11. (a) J. Shi, J. Li, X. J. Huang, and Y. W. Tan, *Nano Res.*, 2011, **4**, 448–459.
(b) I-C. Chang, P.-C. Chen, M.-C. Tsai, T.-T. Chen, M.-H. Yang, H.-T. Chiu and C.-Y. Lee, *Cryst. Eng. Comm.*, 2013, **15**, 2363–2366.

12. (a) H. T. Zhu, J. X. Wang and G. Y. Xu, *Cryst. Growth Des*., 2009, **9**, 633–638. (b) S. Hacialioglu, F. Meng and S. Jin, *Chem. Commun*., 2012, **48**, 1174–1176.
13. (a) Y. M. Sui, Y. Zeng, L. L. Fu, W. T. Zheng, D. M. Li, B. B. Liu and B. Zou, *RSC Adv*., 2013, **3**, 18651–18660. (b) X. Y. Meng, G. H. Tian, Y. J. Chen, Y. Qu, J. Zhou, K. Pan, W. Zhou, G. L. Zhang and H. G. Fu, *RSC Adv*., 2012, **2**, 2875–2881. (c) L.-I. Hung, C.-K. Tsung, W. Y. Huang and P. D. Yang, *Adv. Mater*., 2010, **22**, 1910–1914.
14. (a) L. L. Li, C.N. Nan, Q. Peng and Y. D. Li, Chem. Eur. J. 2012, **18**, 10491–10496. (b) Y. H. Liang, L. Shang, T. Bian, C. Zhou, D. H. Zhang, H. J. Yu**,** H. T. Xu, Z. Shi, T. R. Zhang, L. Z. Wu and C.-H. Tung, *Cryst. Eng. Comm*., 2012, **14**, 4431–4436.
15. Y. Zhang, X. Wang, L. Zeng, S. Y. Song and D. P. Liu, *Dalton Trans.*, 2012, **41**, 4316–4319.
16. S. S. Hafner and S. Nagel, *Phys. Chem. Minerals*, 1983, **9**, 19–22.
17. Q. Kang and Y. G. Zhang, *Green Chem.*, 2012, **14**, 1016–1019.
18. (a) L. Al-Hmoud and C. W. Jones, *J. Catal*., 2013, **301**, 116–124; (b) L. Tang, H. Y. Sun, Y. F. Li, Z. G. Zha and Z. Y. Wang, *Green Chem*., 2012, **14**, 3423–3428.
19. (a) Q. Q. Wang, Y. Q. Deng and F. Shi, *Catal. Sci. Technol*., 2014, **4**, 1710–1715; (b) J. M. Pérez, R. Cano, M. Yus and D. J. Ramón, *Eur. J. Org. Chem*., 2012, 4548–4554.
20. W. J. Cui, Q. Xiao, S. Sarina, W. L. Ao, M. X. Xie, H. Y. Zhu and Z. R. G. T. Bao, *Catal. Today*, 2014, **235**, 152–159.